Rheology of immiscible blends: Relation with structure in transient shear flows

Jan Mewis*, Inge Vinckier and Paula Moldenaers

Department of Chemical Engineering, K.U. Leuven, de Croylaan 46,
B 3001 Leuven, Belgium

SUMMARY: A systematic overview of the behaviour of immiscible blends under various transient flow conditions is presented. On the one hand, it has been observed that the rheological response reflects very clearly the actual microstructure of the blend. It is shown that specific rheological measurements can serve as techniques to probe in-situ and time-resolved the flow-induced blend morphology. On the other hand, models that have been developed to describe the flow behaviour and the corresponding morphology evolution during transient shear flow are discussed. The approach that was used to arrive at these models was to introduce the physics of the morphological processes into the existing black-box model of Doi-Ohta.

Introduction

The transient rheological behaviour of blends is quite different from that of ordinary polymers, because of the contribution of the interface to the stresses. This contribution is closely related to the evolution of the size and shape of the interface. Therefore suitable transient rheological experiments can provide detailed information about the flow-induced structural changes; conversely the transient rheological response can often be predicted quite well from the known evolution of the microstructure. In this paper start-up of flow, a sudden increase in shear rate, cessation of flow and recoil will be discussed, thus providing an overview of possible transient shear histories encountered during processing.

Materials and Methods

All experiments have been performed on a model blend that is liquid at room temperature. Polyisobutene (PIB), produced by Exxon (Parapol 1300), and a polydimethylsiloxane

 CCC 1022-1360/00/$ 17.50+.50/0

(PDMS) from Rhône Poulenc (Rhodorsil 47V200000) have been chosen as model components. Over the shear rate range of interest these components have a nearly constant viscosity of respectively 86 and 195 Pa.s at 23°C. The elasticity of PIB is almost negligible, whereas the PDMS sample displays some elasticity (τ=0.027s). The interfacial tension of this system is 2.3 mN/m [1]. Mixtures of 10% PIB in PDMS as well as the inverse have been tested. The preparation method, the stationary rheological properties and the steady state morphology have been discussed elsewhere[2].

The shear rate controlled measurements have been performed on a Rheometrics Mechanical Spectrometer (RMS 800), equipped with either a 100g.cm or a 2000g.cm force rebalanced transducer. Both transient shear and normal stresses have been recorded. The elastic recovery was measured on a Rheometrics Stress Rheometer (RSR 8600). On both instruments, a cone and plate geometry (diameter of 25mm and 0.1rad cone angle) has been used. For all experiments a well defined experimental protocol ensured well defined initial conditions: the sample was sheared at a low shear rate (or a low shear stress) for a sufficiently long time to obtain a reproducible steady state morphology at the start of the actual experiments.

Results and Discussion

1. Droplet deformation and break-up during flow

This section deals with the response of a blend to inception of flow or, in general, to a stepwise increase in shear rate. When a droplet/matrix system is subjected to a stepwise increase in shear rate the droplets will deform and, when the interfacial stress can no longer resist the hydrodynamic stress, they will disintegrate. The latter condition is satisfied when the capillary number Ca, i.e. the ratio of hydrodynamic over interfacial stress, exceeds a critical value. The corresponding stress transients are very characteristic: after an initial, fast peak the shear stress shows an undershoot which is accompanied by a large overshoot in the first normal stress difference[3,4,5,6]. Examples of such normal stress transients are shown in figure 1.

The peculiar stress responses in figure 1 can be related to the underlying morphological processes by using the approach of Doi and Ohta[7]. The stress tensor σ of a blend is written as the sum of contributions of the component polymers and of the interface. The latter can be correlated with the interface tensor q, expressing the anisotropy of the interface:

$$\sigma = \left(\Phi \cdot \sigma_d + (1-\Phi)\cdot \sigma_m\right) - \alpha \cdot q \qquad (1)$$

where the subscripts d and m refer respectively to the droplet and matrix phases, Φ being the volume fraction of the disperse phase and α the interfacial tension. In eqn (1) a linear mixing rule, based on volume fraction, is used to compute the stress contribution of the pure components. A linear mixing rule has been reported[3] to give a good approximation for the stress contribution of the components when the composition is far from 1:1, as is the case in the present study.

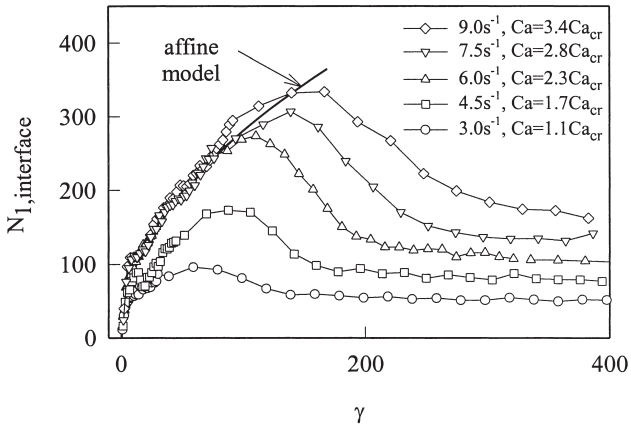

Fig. 1: Evolution of the interfacial contribution to the first normal stress difference for a 10% PDMS in PIB blend after a stepwise increase in shear rate. The initial shear rate was $0.3s^{-1}$; the final shear rate is indicated in the figure. The prediction of eqn. (3) is added for comparison.

Transient stresses can be calculated with eqn (1) once the morphology evolution is known. The original kinetic equations for q of the Doi-Ohta model, however, do not predict adequately the experimentally observed shape of the transient stress curves for droplet/matrix systems. Moreover, these kinetic equations contain two phenomenological parameters, the

values of which are not a priori known. Lee and Park[8] introduced a slightly different phenomenological model which results in a better prediction of the transient shear stress but the agreement with the experimental normal stress transients remains rather poor[9]. Therefore we will use an alternative route to describe the evolution of the stresses, using available results for the deformation of single droplets as a starting point. Interactions between droplets are ignored at this stage.

A general description of the deformation of a droplet immersed in a fluid, subjected to a flow field with a uniform velocity gradient, has been given by Maffettone and Minale[10]. Their only assumption is that the droplet remains ellipsoidal. The evolution of the shape of the droplet after start-up of shear flow can be obtained from their model and inserted in eqn (1) to give the corresponding stress response. However, for high values of the capillary number ($Ca > Ca_{cr}$) the model of Maffettone and Minale diverges. Under the latter conditions, more specifically when the capillary number is more than twice the critical capillary number, it is known that droplets will deform affinely into fibrils, the resulting time-dependent deformation is given by Elemans[11]. In the present study, the shape of the fibril has been approximated by a cylinder with spherical ends to obtain an analytical expression for the shear and normal stress transients after start-up of flow. As soon as the droplet shape can be approximated by a cylinder and up to the point where interfacial instabilities appear, the stresses are given by[6]:

$$\sigma_{12}(t,\dot{\gamma}) = \left(\Phi \cdot \sigma_{12,d} + (1-\Phi)\cdot \sigma_{12,m}\right) + \frac{2\cdot\alpha\cdot\Phi\cdot\left(1+0.5\cdot\gamma^2+0.5\cdot\gamma\cdot\sqrt{\gamma^2+4}\right)^{1/4}}{d_0\cdot\sqrt{\gamma^2+4}} \qquad (2)$$

$$N_1(t,\dot{\gamma}) = \left(\Phi \cdot N_{1,d} + (1-\Phi)\cdot N_{1,m}\right) + \frac{2\cdot\gamma\cdot\alpha\cdot\Phi\cdot\left(1+0.5\cdot\gamma^2+0.5\cdot\gamma\cdot\sqrt{\gamma^2+4}\right)^{1/4}}{d_0\cdot\sqrt{\gamma^2+4}} \qquad (3)$$

where γ is the total strain after the increase in shear rate and d_0 the initial droplet diameter. It should be noticed that these equations do not contain any unknown parameters; the values of the physical quantities, i.e. d_0, α and the component stresses, can be determined experimentally.

The stresses during a stepwise increase in shear rate can be modelled as those in start-up experiments, provided the initial shear rate produces only slightly deformed droplets[6]. This applies to the data in figure 1, which consequently can be used to assess the predictions of

eqns (2) and (3). The interfacial stress contribution, corresponding to the last term in eqn. (3), is displayed in figure 1. Whenever affine deformation can be expected, i.e. $Ca > 2.Ca_{cr}$, the data indeed superimpose when plotted versus strain and obey the model prediction, almost up to the point where the normal stress reaches its maximum. The shear stress can also be predicted quantitatively by this model (not shown), this time until the minimum in the stress curve is reached. Rheo-optical studies on dilute systems[12,13] show that the maximum in anisotropy of the system, which is equivalent to the maximum in normal stress and the minimum in shear stress, coincides with the moment at which interfacial instabilities start to develop. The actual break-up of the fibril occurs somewhat later[13], at the inflection point in the stress curve. This break-up process is obviously not covered by the affine deformation model.

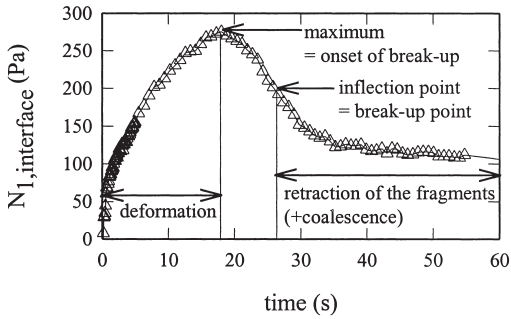

Fig. 2: Schematic representation of the morphological information that can be derived from transient normal stress curves (data of the step-up test from 0.3 to 6.0s^{-1} of figure 1).

The theory of Khakhar and Ottino[14] apparently is the only existing model for fibril break-up during shear flow. Its applicability is limited, however, because it uses as initial condition "the moment at which the fatal disturbance starts to grow", a parameter which is not readily accessible. Very recently, an analysis of the break-up process has lead to a useful scaling property for the break-up time in a particular blend[15]:

$$t_{break} \propto \left(\frac{d_0 \cdot \eta_m}{\alpha} \right)^{2/3} \cdot \dot{\gamma}^{-1/3} \qquad \textbf{(4)}$$

The break-up time t_{break} is defined here as the time elapsed between the onset of shear flow and the moment at which the fibril disintegrates. The proportionality constant, needed to calculate the break-up time with eqn. (4), still depends on the viscosity ratio of the blend[15]. The validity of eqn (4) has been confirmed by rheo-optical experiments[15], and also the present rheologically determined break-up times (inflection points in fig. 1) reflect the shear rate dependence of eqn (4).

Summarizing, it can be stated that stress response due to affine droplet deformation can be predicted quantitatively and the break-up time for various droplet sizes and shear rates can be deduced from the result under one particular test condition. Conversely, the transient rheological response after a stepwise increase in shear rate can be used as an in-situ time resolved probe of the deformation and break-up behaviour of the disperse phase. How this morphological information can be deduced from the transient normal stress curve is schematically indicated in figure 2. The part of the stress curve before the maximum reflects the deformation of the disperse phase. Comparison with the model curve or by comparing stress-strain curves at different high shear rates shows whether the deformation is affine or not. The maximum in normal stress indicates the onset of break-up, i.e. the point at which the anisotropy increase due to stretching is balanced by the loss in anisotropy due to the growth of instabilities. The inflection point in the stress curve is the time at which the fibril actually disintegrates.

2. Retraction and break-up after cessation of flow

In immiscible blends complex relaxational phenomena can occur depending on the aspect ratio of the inclusions[16]. Below a critical aspect ratio the droplet retracts back to a sphere, otherwise the drop will break rather than retract after cessation of flow. For intermediate aspect ratios, break-up will occur by end-pinching, for very extended droplets capillary wave instabilities become the dominant mechanism. The relation between these different mechanisms of structure relaxation and the rheological response will be studied here. The components of the model blends under investigation relax almost instantaneously after cessation of flow; the stresses due to the shape relaxation of the interface relax on a much

longer time scale. Consequently, the stress contribution of the interface, reflecting the morphology evolution, can be clearly isolated.

The relaxation curves of the interfacial stress after stationary shear flow are displayed in figure 3. Under these flow conditions, the morphological processes are relatively simple: the slightly deformed droplet phase retracts back to a sphere. The corresponding interfacial stress contribution to both the shear and the normal stress decays exponentially. Contrary to the behaviour of regular polymers, the time scale for interfacial shear and normal stress relaxation is identical. The exponential stress decay is consistent with the Palierne theory for the linear viscoelastic behaviour of immiscible blends[17]. The experimental time scale, i.e. τ_{relax} in fig. 3, however, deviates already from the linear theory for small droplet deformation. This deviation obeys the following relation[18]:

$$\tau_{relax} = \tau_D \cdot \left(r_p\right)^{2/3} \qquad \textbf{(5)}$$

with τ_D the linear relaxation time predicted by the Palierne model and r_p the aspect ratio of the droplets at the onset of the retraction process.

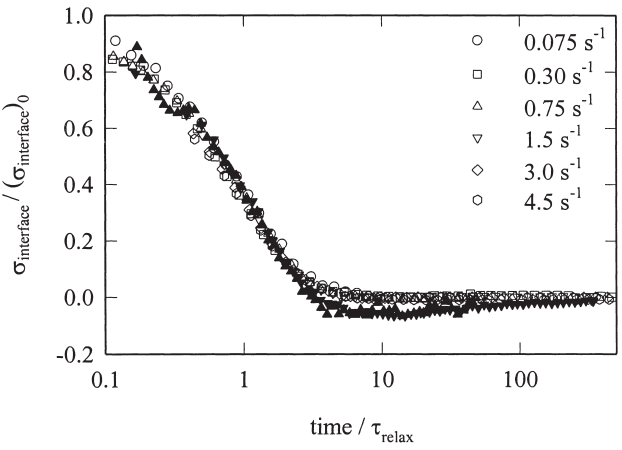

Fig. 3: Scaled stress relaxation curves for 10% PIB in PDMS, obtained after steady shear flow. The interfacial stress contribution to the shear stress and normal stress is indicated by respectively open and filled symbols.

To study the relaxational phenomena of substantially deformed droplets a different transient shear history has been used. As in the experiments discussed above (see 1), a sudden increase in shear rate is applied to a presheared sample. Now, however, the flow is interrupted before break-up sets in. By varying the shearing period, droplets of different shapes can be generated, the relaxation of which is recorded after the flow is arrested. Slightly deformed droplets are obtained when the flow is interrupted very soon after the step-up in shear rate. The longer the sample has been subjected to the high shear rate, the more deformed the disperse phase will be, provided that the break-up has not yet occurred. When the flow is maintained long enough (passing the point of maximum normal stress), the droplets are broken by the flow and again slightly deformed droplets are present in the blend when relaxation starts.

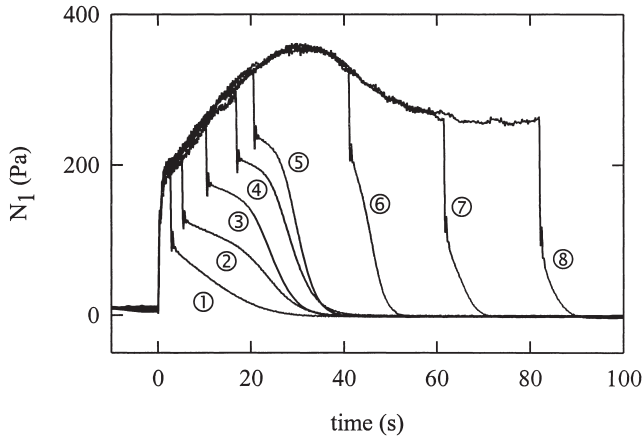

Fig. 4: Normal stress curves of eight different relaxation measurements with an interrupted shear history (step-up from 0.3 to 3.0s^{-1} at time zero) for 10% PIB in PDMS.

Two regions can be distinguished in the normal stress curves after cessation of flow (figure 4): an almost instantaneous stress decay due to the relaxation of the component polymers, followed by a much slower relaxation process driven by interfacial tension. A similar observation can be made for the shear stress (not shown), but there the interfacial stress

contribution is less pronounced. Three different types of interfacial relaxation curves appear in figure 4: an exponential stress decay (curve 8), a non-exponential stress decrease (curve 1) or a relaxation curve with a shoulder (e.g. curve 2). Similar shapes have been encountered for the relaxation of the linear conservative dichroism after the same transient shear histories[12,19]. By comparing the stress profiles with the evolution of light scattering patterns during relaxation[12] and with microscopic observations on single droplets[16], the different shapes for the relaxation curves can be associated with different initial morphologies and the corresponding different mechanisms of shape relaxation. Simple retraction of slightly deformed droplets causes an exponential stress decay, end-pinching which is encountered for rather deformed droplets is reflected in a monotonic, non-exponential stress decrease and break-up of fibrillar structures by sinusoidal instabilities induces a shoulder in the relaxation curve. Consequently, the break-up mechanism and the corresponding time scale can be deduced directly from the experimental stress curves.

As was the case for relaxation after steady shear, the interfacial stress contributions in shear and normal stress relaxation after a transient shear history superimpose when scaled between 1 and 0. This scaling behaviour is consistent with the Doi-Ohta theory[7]. However, a single master curve as in figure 3 can not be obtained by scaling the time axis because of the three different shapes of curves encountered for the different relaxation mechanisms. This complex rheological behaviour during relaxation can not be described by the original Doi-Ohta model[18]. A modified version of this model by Lee and Park[8] can predict exponentially decaying stress curves, but the latter model too fails in describing the relaxation of a fibrillar structure via break-up by sinusoidal instabilities. However, a model for the stress relaxation of a fibrillar morphology can be obtained by combining eqn. (1) with the theory of Tomotika[20], which describes the development of sinusoidal instabilities on the surface of an isolated, infinitely long cylinder. When the evolution of the interface tensor q is calculated with the Tomotika theory, the resulting stress curve has indeed a shoulder[18]. The calculated relaxation, however, starts with a horizontal plateau, whereas the experimental curve starts with a steady decrease. This discrepancy can be attributed to the fact that the disperse phase does not consist of infinitely long cylinders but of fibrils with a large, but finite, aspect ratio. These begin to retract and break via end-pinching until the capillary wave instabilities cause an abrupt break-up of the remaining thread. The combined occurrence of end-pinching and sinusoidal

instabilities has been observed directly by microscopy[16] and also shows up in dichroism measurements during relaxation[12].

As a result, two characteristic times appear in the stress relaxation curves: one describing the initial decrease caused by end-pinching and a second one for the decay after the shoulder resulting from for the amplitude growth of the distortions. The latter characteristic time can be predicted from the Tomotika model[20]:

$$t_{break} = \frac{2 \cdot \eta_m \cdot R_0}{\alpha \cdot \Omega(p)} \cdot \ln\left(\frac{0.81 \cdot R_0}{A_0}\right) \tag{6}$$

with R_0 being the fibril radius, A_0 the a priori unknown initial amplitude of the disturbance and $\Omega(p)$ a known function of the viscosity ratio. Although two different mechanisms contribute to the stress relaxation, the curves in figure 4 that display a shoulder can be superimposed by scaling the time axis with one single characteristic time τ_{RI}[18]:

$$\tau_{RI} = \frac{2 \cdot \eta_m \cdot R_0}{\alpha \cdot \Omega(p)} \tag{7}$$

This scaling behaviour indicates that the second factor in eqn. (6) does not vary much under the experimental conditions of figure 4. More importantly, it also shows that the dominating time scale for relaxation of a fibrillar structure is that of break-up by interfacial instabilities, even though end-pinching occurs in the initial stages of the relaxation process.

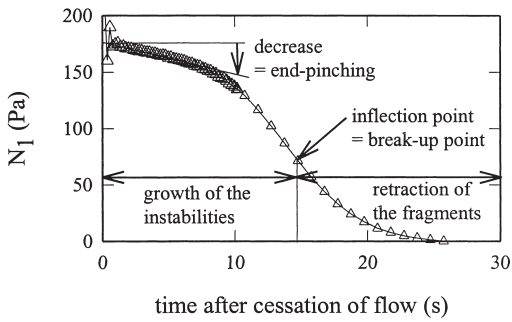

Fig. 5: Morphological information that can be derived from normal stress relaxation curves (example for curve 3 of figure 4).

In summary, one can conclude that the stress relaxation after cessation of flow can be modelled. The stress due to simple droplet retraction can be predicted quantitatively by a modification of the linear relaxation time of the Palierne model; the main features of the stress relaxation curves caused by a disintegrating fibril can be deduced from a combination of the Doi-Ohta approach with the Tomotika theory. Conversely, the stress relaxation curves can be used to probe the flow-induced morphological processes: both the mechanism of shape relaxation of the disperse phase and the corresponding time scale can be deduced directly from the rheological measurement. This is illustrated in figure 5 for the case of relaxation of a fibrillar structure: the shoulder in the relaxation curve is characteristic for the growth of sinusoidal instabilities and the inflection point directly indicates the time needed for fibril break-up by this process.

3. Elastic recovery

In this last section, the effect of the underlying morphological processes on elastic recovery will be investigated. The elastic recovery experiment is complementary to the stress relaxation discussed in the previous section: both phenomena are caused by the shape relaxation of the droplet phase but the boundary conditions differ. In recoil tests, the stress on the sample is suddenly removed; in stress relaxation experiments the flow is suddenly arrested. The recovery after steady shear flow will be discussed first, followed by a summary of the recoil after a transient shear history.

The elastic recovery curves after steady state shearing at 100Pa and 200 Pa are displayed on figure 6 as dashed lines. This preshear generates a slightly deformed blend morphology with a droplet size inversely proportional to the applied stress. As the component polymers show hardly any recoil under the stresses applied in these tests, the measured recovery can be attributed completely to the retraction of the deformed droplets. It was observed that after sufficiently long shearing periods, the ultimate recovered strain is independent of the applied stress, only the time scale of recoil is affected by the stress level. Qualitatively, this behaviour can be deduced[21] from the Doi-Ohta model. The characteristic time for recoil can be derived from the Palierne model; non-linear deformation effects can again be taken into account by

multiplying the Palierne retardation time by the aspect ratio of the droplet phase to the power 2/3. The prediction for the elastic recovery γ_r of a blend with Newtonian components then becomes[21]:

$$\gamma_r(t) = \frac{\sigma_{12} \cdot (\tau_1 - \tau_2)}{\eta_0} \cdot \left(1 - \exp\left(\frac{-t}{\tau_2 \cdot r_p^{2/3}} \right) \right) \qquad (8)$$

where σ_{12} is the applied shear stress. The expressions to be used for the blend viscosity η_0 and for the relaxation and retardation time (τ_1 and τ_2) are those of the Palierne model. These two characteristic times are proportional to the droplet size. Hence a constant final recoil level is predicted for blends in which the droplet size is inversely proportional to the applied shear stress, as was the case for the two dashed curves of figure 6.

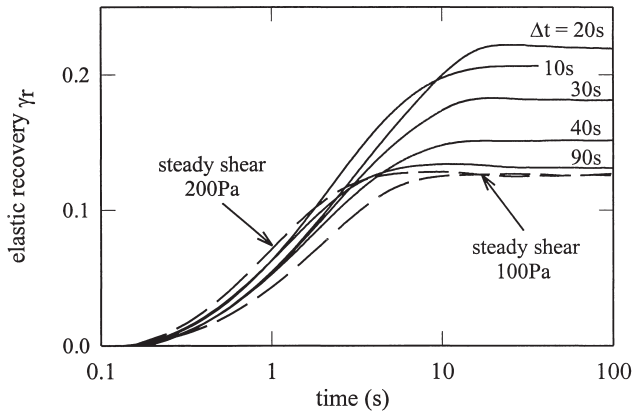

Fig. 6: Elastic recovery of 10%PIB in PDMS after a transient shear history consisting of a stepwise increase in stress from 100 to 200Pa. The stress (200 Pa) was removed after a limited time (Δt as indicated on the figure). The recovery curves after steady state shearing at respectively 100 and 200Pa are added for reference.

In a second series of experiments, the recoil of a more deformed morphology is investigated. A transient shear history is applied consisting of initial shearing at a low stress, followed by a sudden jump to a higher stress level. Releasing the stress before the steady state morphology at the high stress level has been reached, results in a more complex elastic recovery. It can be substantially larger and slower than the one corresponding to a steady state preshear (see figure 6). In these tests, the recoil behaviour depends on both the instantaneous structure at the onset of the recoil and on the morphological changes during recovery. Consequently, these

recoil curves can also be used to probe the underlying morphological processes. It can be shown that an increasing level of recoil corresponds to an initial morphology that is more deformed but is still able to retract without breaking during recoil; a decrease of the final recovery level is obtained when highly elongated fibrils were generated which disintegrate during the subsequent recovery process[22].

Finally, it should be mentioned that these "transient" recoil experiments show a close correspondence to the relaxation after an equivalent rate-controlled shear history, i.e. a step-up in shear rate. The same morphological processes, such as fibril break-up, occur during both recoil and relaxation. Due to this similarity, the recovery curves can be approximately calculated from the equivalent transient relaxation experiments[22].

Conclusions

The transient behaviour of immiscible model blends has been investigated under specific flow conditions, which represent aspects of processing flows. Physical models and scaling relations have been presented to describe the morphology evolution and the corresponding transient stresses in semi-dilute systems. As long as the droplet deformation of the disperse phase remains moderate, linear viscoelastic theories can be applied, although a modification of the characteristic time scale is necessary to fit the experimental data. Models for more deformed structures can be obtained by introducing the physics of the morphological processes involved, e.g. single droplet deformation theories, into the black-box model of Doi-Ohta. This approach resulted in a description of the rheological response caused by droplet deformation and break-up during flow and by shape relaxation after either cessation of flow or under recoil conditions.

It has also been shown that rheological measurements provide a means to probe flow-induced morphological changes, such as droplet deformation, retraction and different mechanisms of break-up, as well as the corresponding time scales.

Acknowledgments – This work was supported in part by the European Community (contract BRE2.CT92.0213), Onderzoeksfonds K.U.Leuven (GOA nr. 98/06) and FKFO (Belgium). Inge Vinckier is indebted to the FWO-Vlaanderen for a post-doctoral fellowship.

References

1. D. Rusu, PhD thesis, Ecole Nationale Superieure des Mines de Paris, Sophia Antipolis, France (1997).
2. I. Vinckier, P. Moldenaers and J. Mewis, *J. Rheol.* **40**, 613 (1996)
3. Y. Takahashi, S. Kitade, N. Kurashima and I. Noda, *Polymer J.* **26**, 1206 (1994)
4. Y. Takahashi, N. Kurashima, I. Noda and M. Doi, *J. Rheol.* **38**, 699 (1994)
5. G.K. Guenther and D.G. Baird, *J. Rheol.* **40**, 1 (1996)
6. I. Vinckier, P. Moldenaers and J. Mewis, *J. Rheol.* **41**, 705 (1997)
7. M. Doi and T. Ohta, *J. Chem. Phys.* **95**, 1242 (1991)
8. H.M. Lee and O.O. Park, *J. Rheol.* **38**, 1405 (1994)
9. O.O. Park and H.M. Lee, Proc. XIIth PPS Meeting, Sorrento, pp. 191 (1996)
10. P.L. Maffetone and M. Minale, *J. Non-Newtonian Fluid Mech.* **78**, 227 (1998)
11. P.H.M. Elemans,H.L. Bos, J.M.H. Janssen and H.E.H. Meijer, *Chem. Eng. Sci.* **48**, 267 (1993)
12. H. Yang, H. Zhang, P. Moldenaers and J. Mewis, *Polymer* **39**, 5731 (1998)
13. J. Vermant, P. Van Puyvelde, P. Moldenaers, J. Mewis and G.G. Fuller, *Langmuir* **14**, 1612 (1998)
14. D.V. Khakhar and J.M. Ottino, *Int. J. Multiphase Flow* **13**, 71 (1987)
15. P. Van Puyvelde, H. Yang, P. Moldenaers and J. Mewis, *Rheol. Acta*, submitted (1999)
16. H.A. Stone, B.J. Bentley and L.G. Leal, *J. Fluid Mech.* **173**, 131 (1986)
17. J.F. Palierne, *Rheol. Acta* **29**, 204 (1990)
18. I. Vinckier, J. Mewis and P. Moldenaers, *Rheol. Acta* **36**, 512 (1997)
19. P. Van Puyvelde, H. Yang, J. Mewis and P. Moldenaers, *J. Colloid Int. Sci.* **200**, 86 (1998)
20. S. Tomotika, *Proc. Roy. Soc. (London)* **A150**, 322 (1935)
21. I. Vinckier, P. Moldenaers and J. Mewis, *Rheol. Acta* **38**, 65 (1999)
22. I. Vinckier, J. Mewis and P. Moldenaers, *Rheol. Acta*, in press (1999)